

# Assessing Fiber Tracking Accuracy via Diffusion Tensor Software Models

Sebastiano Barbieri<sup>a</sup>, Jan Klein<sup>a</sup>, Christopher Nimsky<sup>b</sup>, and Horst K. Hahn<sup>a</sup>

<sup>a</sup>Fraunhofer MEVIS - Institute for Medical Image Computing,  
Universitätsallee 29, 28359 Bremen, Germany;

<sup>b</sup>Department of Neurosurgery, University of Marburg,  
Baldingerstrasse, 35033 Marburg, Germany

## ABSTRACT

In the last few years, clinicians have started using fiber tracking algorithms for pre- and intraoperative neurosurgical planning. In the absence of a ground truth, it is often difficult to assess the validity and precision of these algorithms. To this end, we develop a realistic DTI software model in which multiple fiber bundles and their geometrical configuration may be specified, also allowing for scenarios in which fiber bundles cross or kiss and which are common bottlenecks of fiber tracking algorithms. Partial voluming, that is the contributions of multiple tissues to a voxel, is taken into account. The model gives us the possibility to compute the diffusion-weighted signal attenuation given certain tissue and scanner parameters. On the tissue side we can model the diffusion coefficients, the principal diffusion direction and the width of the fiber bundles. On the scanner side, we can model the diffusion time, the strength and direction of the applied diffusion gradient and the width of the diffusion pulse. We also include the possibility to add noise and various artifacts such as aliasing and  $N/2$  ghosting to the model. Having generated the model of a fiber bundle, we determine the distance between the tracked fibers and the original model, thus being able to make assertions on the accuracy of the employed fiber tracking algorithm. Moreover, we can use this information to give an indication about an appropriate width of a safety margin around the tracked fiber bundle.

**Keywords:** Brain, Diffusion Tensor Imaging, Fiber Tracking, Noise, Artifacts, Software Model, Safety Margin

## 1. INTRODUCTION

Diffusion tensor imaging (DTI) is a magnetic resonance imaging method which allows to measure the anisotropic diffusion of water molecules in in-vivo biological tissue, such as white matter (WM), in the brain. An important application of DTI is fiber tractography, which assumes that the principal diffusion direction matches the orientation of the corresponding underlying fiber system and thus allows the reconstruction of the 3D architecture of WM fiber pathways. In recent years fiber tractography has become well established in the research environment, with several clinical uses being reported.

One of the major hurdles when developing fiber tracking algorithms is that hardware or software models of fiber bundles are needed in order to assess their validity and precision. It is therefore necessary to develop hardware or software models with a known fiber network. Software models have the advantage that they can be easily modified to account for different scanner parameters, image noise or artifacts. While much of the previous work has focused on simple models in which fiber bundles were represented as cylindrical tubes or helices (see for example<sup>1-3</sup>), in this work we suggest a framework in which it is possible to simulate both the smooth transition between the actual white matter pathway and the surrounding tissue and the partial volume effects caused by the possible contemporary presence of white

---

Further author information: (Send correspondence to Sebastiano Barbieri)

Sebastiano Barbieri: E-mail: [sebastiano.barbieri@mevis.fraunhofer.de](mailto:sebastiano.barbieri@mevis.fraunhofer.de), Telephone: +49 (0)421 218 8164

Jan Klein: E-mail: [jan.klein@mevis.fraunhofer.de](mailto:jan.klein@mevis.fraunhofer.de), Telephone: +49 (0)421 218 8902

Christopher Nimsky: E-mail: [nimsky@med.uni-marburg.de](mailto:nimsky@med.uni-marburg.de), Telephone: +49 (0)6421 586 6447

Horst K. Hahn: E-mail: [horst.hahn@mevis.fraunhofer.de](mailto:horst.hahn@mevis.fraunhofer.de), Telephone: +49 (0)421 218 9183

matter, grey matter and cerebrospinal fluid in one voxel. Even though we only model fiber bundles with a circular cross section, in many cases this restriction is lifted by the actual presence of white matter at a cross section. We realistically simulate the noise in magnetic resonance scans and image artifacts such as aliasing and  $N/2$  ghosting.

We focus on generating a phantom of the corticospinal tract. Afterwards, we reconstruct the modeled tract by means of a fiber tracking algorithm and make a quantitative analysis of the algorithm’s accuracy. This information is used to estimate what an appropriate safety margin around the tracked fibers should be and to analyze after which length the first fibers start to leave the modeled fiber bundle.

## 2. METHODS

In this section, we start by introducing the general framework that we use to generate the diffusion tensor model. Next, we provide details on how we model different tissues and white matter pathways. After a brief overview of the employed fiber tracking algorithm, we conclude with an analysis of its accuracy.

### 2.1 DTI Model Framework

In order to generate a synthetic tensor field, we start by computing a set a of diffusion-weighted (DW) images (one image for each corresponding gradient direction).

The diffusion-weighted signal is modeled according to the CHARMED model proposed in.<sup>4,5</sup> This model contains a hindered extra-axonal compartment as well as a restricted intra-axonal compartment. We restrict ourselves to the hindered model, which gives rise to an effective diffusion tensor and primarily explains the Gaussian signal attenuation observed at low  $b$  values. Let us denote the diffusion time by  $\Delta$  and set

$$\mathbf{q} = \frac{\gamma \mathbf{g} \delta}{2\pi}$$

Here  $\gamma$  is the proton gyromagnetic ratio,  $\mathbf{g}$  is the vector whose magnitude is the strength of the applied diffusion gradient and whose direction is along the axis of the applied diffusion gradient,  $\delta$  is the width of the diffusion pulse gradient. In this case, the net signal attenuation is given by

$$E(\mathbf{q}, \Delta) = \sum_{i=1}^M f_h^i \cdot E_h^i(\mathbf{q}, \Delta) \quad (1)$$

where the  $f_h^i$  are the  $T_2$  weighted volume fractions of the hindered compartments,  $E_h^i(\mathbf{q}, \Delta)$  is the normalized MR echo signal from the  $i$ -th hindered compartment in a voxel. The CHARMED model assumes a cylindrically symmetric tensor model ( $\lambda_1 \neq \lambda_2 = \lambda_3$ ) and denotes the diffusion coefficients parallel and perpendicular to the axon’s fiber by  $\lambda_{\parallel}$  and  $\lambda_{\perp}$  respectively. In similar manner,  $q$  may be written as  $\mathbf{q} = \mathbf{q}_{\parallel} + \mathbf{q}_{\perp}$ . For details on the computation of  $\mathbf{q}_{\parallel}$  and  $\mathbf{q}_{\perp}$  see [4, Appendix B]. Then  $E_h^i(\mathbf{q}, \Delta)$  is given by

$$E_h^i(\mathbf{q}, \Delta) = e^{-4\pi^2(\Delta - (\delta/3))|q_{\parallel}|^2\lambda_{\parallel}} + e^{-4\pi^2(\Delta - (\delta/3))|q_{\perp}|^2\lambda_{\perp}}$$

It is known that noise in magnitude magnetic resonance data is Rician distributed.<sup>6</sup> As suggested in,<sup>7</sup> such noise distribution may be simulated in the image by computing  $|E(\mathbf{q}, \Delta) + \tilde{N}(0, \sigma^2)|$ , where  $\tilde{N}(0, \sigma^2)$  is a Gaussian distributed complex variable with mean 0 and variance  $\sigma^2$ . Using standard fitting procedures, we use the DW images to compute the tensor valued image.

### 2.2 Generating the BrainWeb-Based Model

Given the framework presented in Section 2.1, we need to specify the fractions of tissue present in each voxel with the corresponding  $T_2$  and diffusion properties. To this end, we build upon the BrainWeb project at McGill University.<sup>8,18</sup> The BrainWeb project provides a dataset created by means of 27 low-noise scans ( $T_1$  weighted gradient echo acquisitions with TR/TE/FA = 18ms/10ms/30°) of the same individual, coregistered in stereotaxic space where they were subsampled and intensity averaged.<sup>9</sup> By means of a modified minimum-distance classifier, ten volumetric datasets that define the spatial distribution for different tissues were created. In these images, the voxel intensity is proportional to the fraction of

tissue within the voxel. In our model we make use of the white matter, grey matter and cerebrospinal fluid volumes, an example slice of each volume is shown in Figure 1. The volumes are defined at a 1mm isotropic voxel grid, with dimensions 181×217×181 (X×Y×Z). Other tissue volumes that might be included in our model in later work include fat, skin, glial matter, and connective tissue.

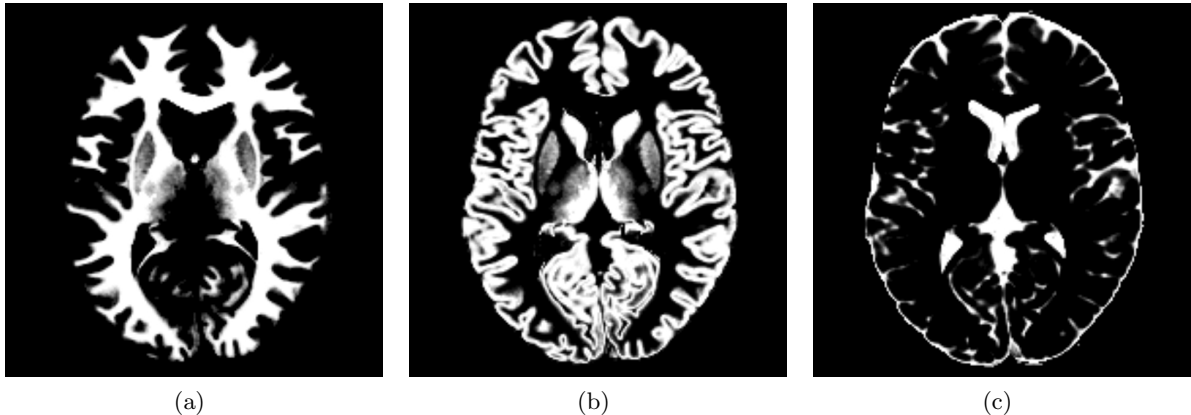


Figure 1. (a): An example slice of the white matter volume. (b): The grey matter volume. (c): The cerebrospinal fluid volume.

To each fraction of tissue in a voxel we assign a main diffusion direction and the eigenvalues of the cylindrically symmetric diffusion tensor. The resulting signal attenuation is then computed according to Equation 1. For the above tissues, the average eigenvalues of the diffusion tensors have been measured and reported in,<sup>10–12</sup> from which we derive the eigenvalues for our model written in Table 1. In case

|                     | $T_2$ (ms) | $\lambda_{\parallel}$ ( $10^{-4}\text{mm}^2/\text{s}$ ) | $\lambda_{\perp}$ ( $10^{-4}\text{mm}^2/\text{s}$ ) |
|---------------------|------------|---|---|
| White Matter        | 70         | $11.30\pm 0.7$  | $5.15\pm 0.3$                                       |
| Grey Matter         | 83         | $9.90\pm 0.4$   | $7.05\pm 0.3$                                       |
| Cerebrospinal Fluid | 329        | $36.00\pm 2.3$  | $30.36\pm 1.8$                                      |

Table 1.  $T_2$  values and tensor eigenvalues used in the BrainWeb-based model for the different tissues.

we do not model one or more white matter tracts to go through a voxel  $V$ , we assign a random main diffusion direction to each tissue portion present in  $V$ . However, we let the main diffusion directions corresponding to a given tissue type vary smoothly in space, in order to have, at least locally, a realistic change in tensor orientation.

Otherwise, if  $V$  has a white matter tissue portion and there are one or more fiber bundles going through it, the main diffusion direction depends on these bundles. Details on the modeling of fiber bundles and on setting the main diffusion direction are given in the following Section 2.3.

## 2.3 Modeling White Matter Pathways

In order to model a white matter pathway we start by defining a tuple of  $n$  control points  $\{P_i\}_{i=1,\dots,n}$  in  $\mathbb{R}^3$  through which the fiber bundle should go. To obtain a smooth backbone of a fiber bundle from just a few control points, we perform cubic spline interpolation on  $\{P_i\}$ . For simplicity we choose Catmull-Rom splines, which are defined by two points  $P_i, P_{i+1}$  and two tangent vectors  $T_i, T_{i+1}$ . The tangent vectors are computed by

$$T_j = \frac{1}{2} \cdot (T_{j+1} - T_{j-1})$$

Then the evolution of the parametric curve  $s_i(t) = (x_i(t), y_i(t), z_i(t))^T$  with  $t \in [0, 1]$  and connecting  $P_i$  and  $P_{i+1}$  is given for example in  $x$ -dimension by

$$x_i(t) = \begin{pmatrix} t^3 & t^2 & t & 1 \end{pmatrix} \cdot \begin{pmatrix} 2 & -2 & 1 & 1 \\ -3 & 3 & -2 & -1 \\ 0 & 0 & 1 & 0 \\ 1 & 0 & 0 & 0 \end{pmatrix} \cdot \begin{pmatrix} P_{i_x} \\ P_{i+1_x} \\ T_{i_x} \\ T_{i+1_x} \end{pmatrix}$$

and similarly in the other dimensions. Concatenating the different splines  $\{s_i\}$  we have a differential 3D curve  $s$  connecting  $P_1$  to  $P_n$ . See Fig. 2(a) for an example curve.

Next, we resample the spline  $s$  at (small) equidistant  $t$  steps and obtain a final set of points which we denote by  $\{r_i\}_{i=1,\dots,N}$ . As suggested in,<sup>13</sup> we define a piecewise differential 3D space curve  $t(r)$ , which is 1 if  $r$  is on the backbone of the fiber and 0 else.  $t(r)$  is given by

$$t(r) = \sum_{i=1}^{N-1} \int_0^1 \delta[r - (r_i + \alpha\Delta_i)] d\alpha$$

where  $\delta$  denotes the Dirac-delta distribution and  $\alpha$  is a parametrization variable. To model the non-constant fiber density we convolve the fiber trajectory  $t(r)$  with a kernel  $k(r)$ :

$$T(r) = t(r) * k(r) = \sum_{i=1}^{N-1} \underbrace{\int_0^1 k[r - (r_i + \alpha\Delta_i)] d\alpha}_{\equiv T^i(r)}$$

Specifically we choose the saturated kernel

$$k(r) = \frac{\operatorname{erf}\left(\frac{w+2\|r\|}{2\sqrt{2}\sigma}\right) + \operatorname{erf}\left(\frac{w-2\|r\|}{2\sqrt{2}\sigma}\right)}{2 \operatorname{erf}\left(\frac{w}{2\sqrt{2}\sigma}\right)}$$

where  $\operatorname{erf}$  is the error function, the parameter  $w$  controls the width of the fiber bundle and  $\sigma$  controls the variance of the Gaussian decay.

We set the percentage  $P(r)$  of white matter occupied by the fiber in the voxel at  $r$  by

$$P(r) = \frac{T(r)}{\max_{r \in \mathbb{R}^3} T(r)}$$

The remaining white matter is modeled as having a random direction. In case there are several fibers which contribute to a voxel, we generally proceed as above, with the difference that we may have to rescale each contribution by the sum of all contributions, so that the latter sum is less or equal to one (100%).

The main diffusion direction  $e_1$  of a fiber at  $r$  is computed as a weighted sum of the vector lines  $\Delta_i$ :

$$e_1(r) = \frac{\sum_{i=1}^{N-1} T^i(r) \Delta_i}{\left\| \sum_{i=1}^{N-1} T^i(r) \Delta_i \right\|}$$

A schematic representation of the main diffusion directions of the tensors is given in Fig. 2(b). Figure 3 shows an example fiber and two crossing fibers with and without random “background” directions.

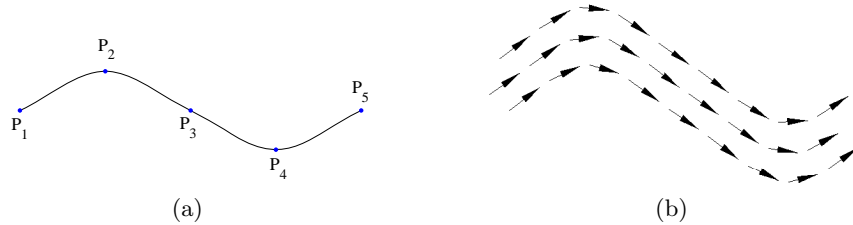


Figure 2. (a): Example curve interpolating the control points  $\{P_i\}$  and forming the backbone of the modeled fiber bundle. (b): Schematic representation of the main diffusion directions of the tensors within the modeled fiber bundle.

## 2.4 Noise, Aliasing, and N/2 Ghosting

In our model, we add Rice distributed noise to the diffusion weighted images as described in Section 2.1. The variance of the noise may be computed as illustrated in<sup>14,17</sup> through

$$\sigma^2 = K \frac{N_x N_y \langle V^2 \rangle}{N_{av} \text{FOV}_x^2 \text{FOV}_y^2 \Delta_t}$$

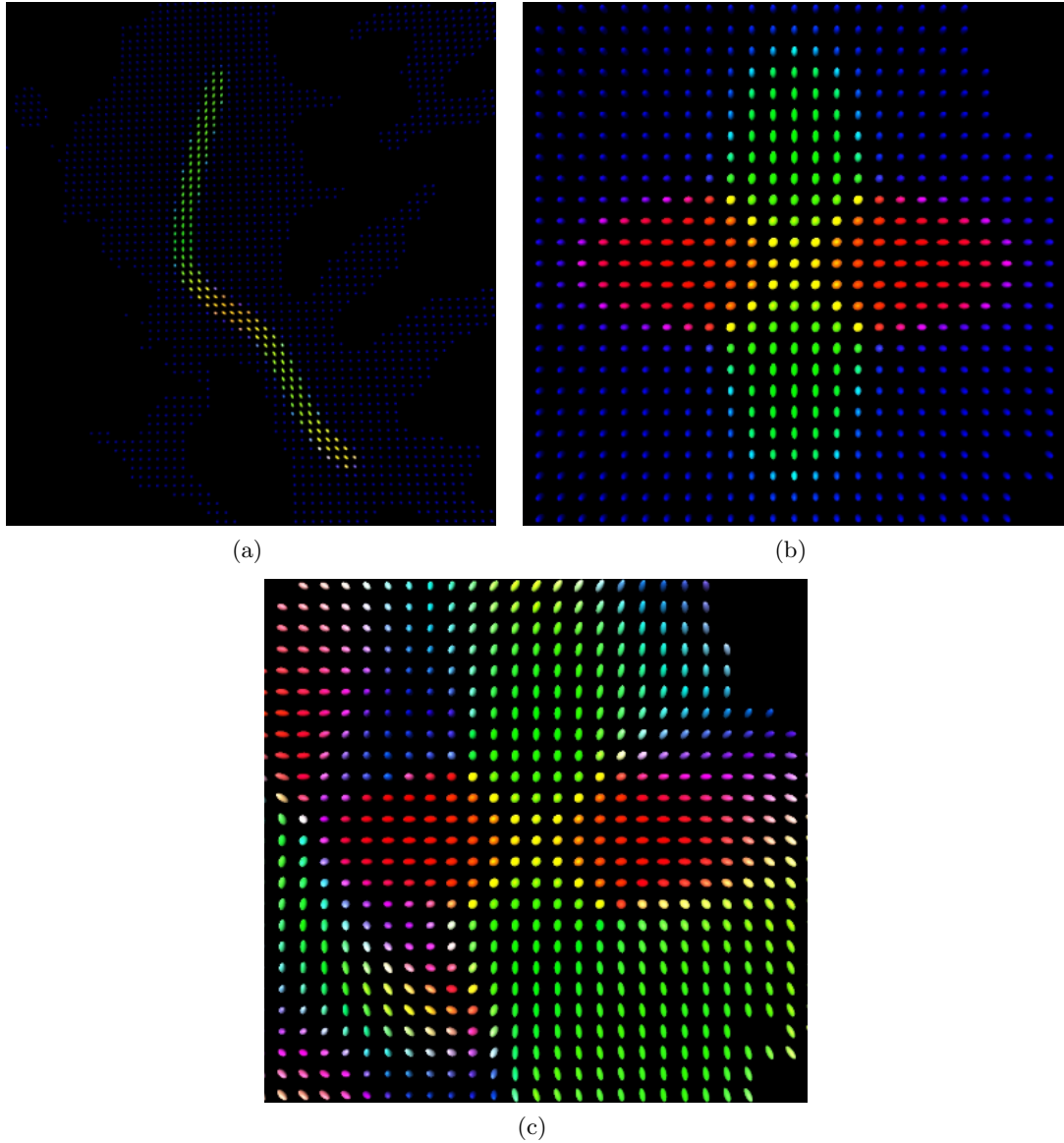


Figure 3. (a): Example fiber. (b): Two crossing fibers without random “background” directions. (c): Two crossing fibers with random “background” directions.

where  $N_x, N_y$  are the number of samples in  $x$  and  $y$  direction,  $\langle V^2 \rangle$  is the thermal noise power,  $N_{av}$  is the number of averages,  $FOV_x, FOV_y$  are the fields of view in  $x$  and  $y$  direction,  $\Delta_t$  is the sampling interval and  $K$  is a scanner depended factor.

As far as artifacts in magnetic resonance images are concerned, two frequent ones are aliasing and  $N/2$  ghosting. Aliasing is caused by a field of view smaller than the anatomy being imaged: it occurs in phase encoding direction, and in case of three dimensional acquisition, it may also occur in section direction. For a given slice of the BrainWeb based model, we simulate aliasing as follows. We add an intensity scaled copy of the image voxels with  $y$ -coordinate larger or smaller than the field of view in  $y$ -direction, at the bottom or at the top of the image, respectively.  $N/2$  ghosting is an artifact caused by phase errors in  $k$ -space. On images acquired with a single-shot echo-planar imaging sequence, the ghost appears as an additional image with reduced intensity that is shifted by half the field of view.<sup>15</sup> This artifacts is thus simply modeled by adding an intensity scaled version of our image shifted by half the field of view. For both presented artifacts, we use scaling factors in the range  $(0, 1)$ . Figure 4 shows some examples of simulated images with noise and artifacts.

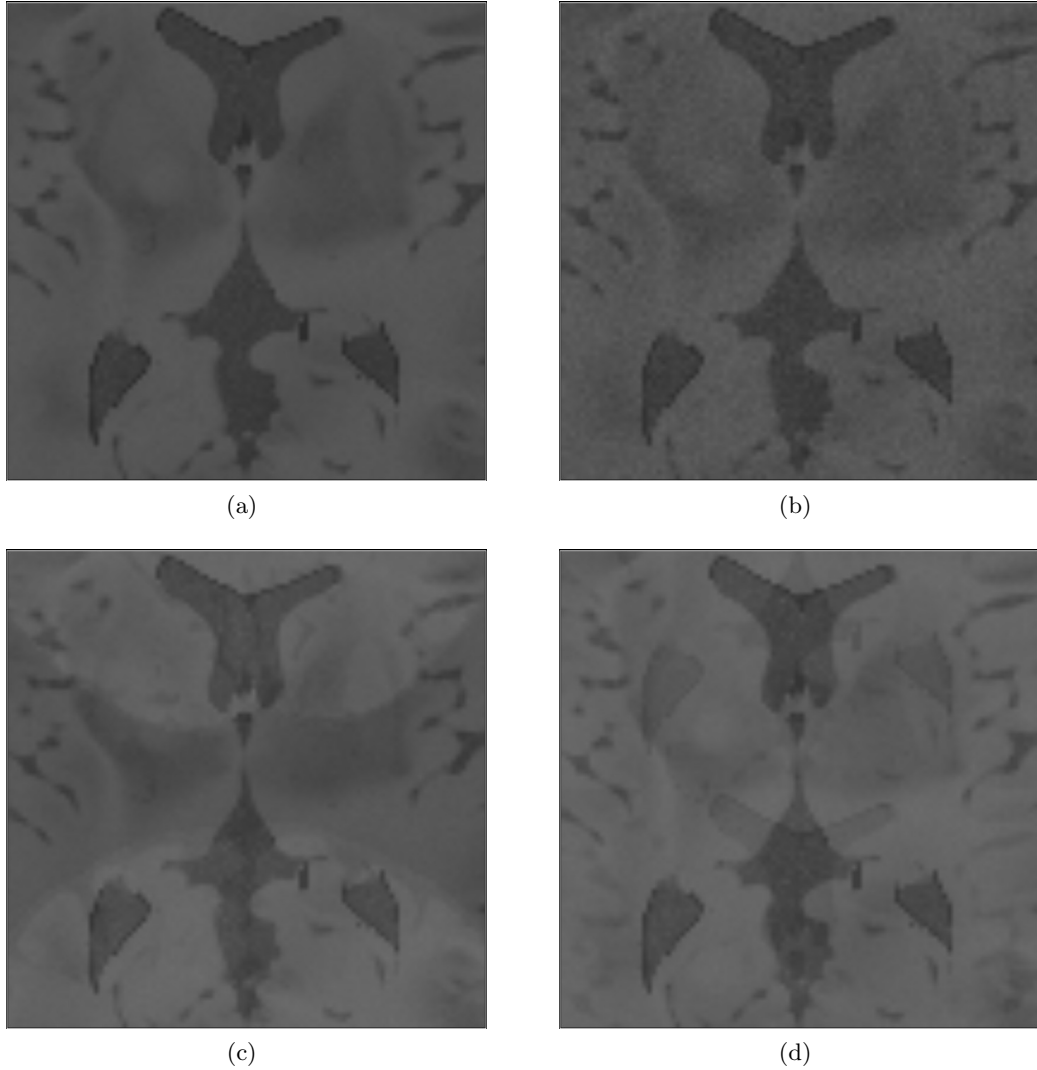


Figure 4. (a): Example slice of a modeled diffusion weighted image, with gradient pointing in  $x$  direction. (b): Complex Gaussian noise with  $\sigma^2=80$  added to the image. (c): Aliasing with factor=0.4 added to the image. (d):  $N/2$  ghosting with factor=0.4 added to the image.

## 2.5 Fiber Tracking Analysis

With the help of a physician having experience with DTI, we define the backbone of the right corticospinal tract. It is initially defined by 18 points and the parameters for the convolution kernel are  $w=12\text{mm}$  and  $\sigma=0.5$ . After resampling it consists of 968 points at a distance of 0.1mm. It is important to note that the thickness of a fiber bundle does not only depend on the kernel width, but also on the actual presence of white matter in the different voxels. After the fiber has been added to the model, we track it using the advection-diffusion based fiber tracking algorithm presented in.<sup>16</sup> For a given tracking position  $r^t$  and step length  $\Delta s$  the next position  $r^{t+1}$  is given by

$$r^{t+1} = r^t + \mathbf{d}^t \Delta s + \frac{1}{2} \mathbf{k}^t \Delta s^2$$

$\mathbf{d}^t$  is computed by using the previous tracking direction  $\mathbf{d}^{t-1}$

$$\mathbf{d}' = \left[ \alpha \mathbf{v} \mathbf{v}^t + (1 - \alpha) \frac{\mathbf{D}}{\lambda_{\max}} \right] \mathbf{d}^{t-1} \quad \mathbf{d}^t = \frac{\mathbf{d}'}{\|\mathbf{d}'\|}$$

here,  $\mathbf{D}$  is the tensor at  $\mathbf{r}^t$  with largest eigenvalue  $\lambda_{\max}$  and corresponding eigenvector  $\mathbf{v}$ , the weight  $\alpha \in [0, 1]$  interpolates between streamline ( $\alpha = 1$ ) and deflection ( $\alpha = 0$ ) based tracking. Further,  $\mathbf{k}^t$  is a curvature term given by

$$\mathbf{k}^t = \frac{\mathbf{d}^t - \mathbf{d}^{t-1}}{\Delta s}$$

which helps improving fiber tracking accuracy.

In our implementation, the resulting tracked fibers are represented by several linearly connected points. To evaluate our algorithm, we compute the Hausdorff distance between one point of the spline-interpolated fiber backbone and the points of the tracked fibers. Given that the fibers are sampled densely enough, this distance provides a good approximation of the maximal distance between the fibers in the model and those that are tracked.

### 3. RESULTS

The remaining parameters used to compute the diffusion weighted images according to Equation 1 are reported in Table 2. We select a region at the level of the internal capsule to start the tracking of the

|                            | Default value                      |
|----------------------------|------------------------------------|
| voxel size                 | $1 \times 1 \times 1 \text{ mm}^3$ |
| number of gradients        | 6                                  |
| gradient strength          | 20 T/m                             |
| diffusion time             | 40 msec                            |
| pulse width                | 35 msec                            |
| gyromagnetic ratio         | $2.675 \cdot 10^8 \text{ rad/sT}$  |
| thermal noise variance     | 100                                |
| fiber tracking step length | 1 mm                               |

Table 2. Parameters used to compute the signal attenuation.

corticospinal tract. After the tracking, fibers which are obviously not part of the corticospinal tract are excluded from the result. Figure 6 shows the tracked fibers and the distance plot. More in detail, the plot shows on one hand the maximum distance between fiber backbone and tracked fibers, on the other the minimum distance between fibers correctly tracked inside the bundle and the border of the bundle model (note that in the midbrain the latter distance may also be constrained by the actual presence of white matter).

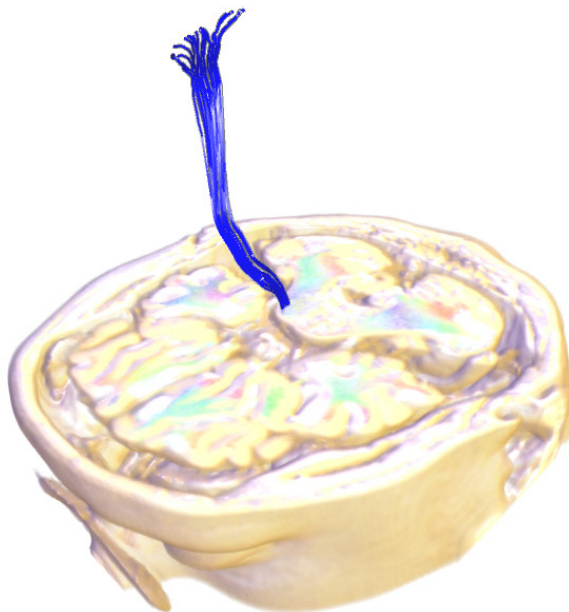


Figure 5. Fiber tracking based on our DTI software model, anatomy given by the BrainWeb phantom.

We observe that fibers are tracked correctly inside the modeled fiber bundle between 3.5 and 48mm. Given that the fiber tracking seed was close to 25mm, this indicates that after a distance of approximately 20mm the first fibers leave the modeled bundle. When fibers are tracked correctly inside the bundle, the

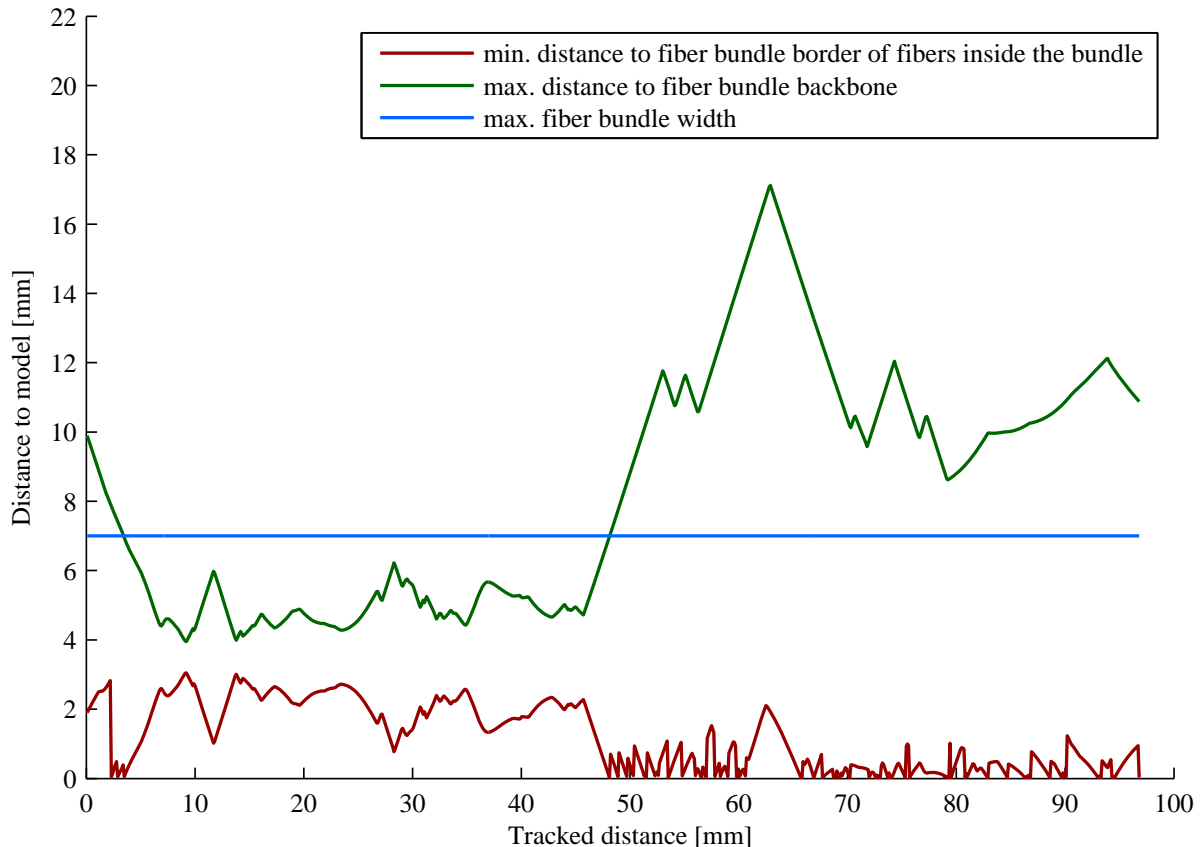


Figure 6. Maximum distance between tracked fibers and modeled fiber bundle backbone.

maximum distance to the fiber bundle border varies between 2 and 3mm, which this experiment indicates to be an appropriate safety margin.

## 4. CONCLUSIONS

In this paper, we make a further step towards the creation of realistic DTI software models. These can be used as ground truth to test various fiber tracking algorithms. A first quantitative analysis of the advection-diffusion based fiber tracking algorithm suggests that, in the considered experiment, the first fibers leave the modeled bundle after approximately 20mm and that a safety margin of 2-3mm seems appropriate. Future work includes analyzing the precision of the algorithm in the presence of kissing or crossing fibers. We would also like to systematically analyze how precision varies in relation with the underlying image data (testing different values for image noise or artifacts, thickness of the fiber bundle, fractional anisotropy of the tensors) or in relation with fiber tracking parameters (such as step length, density of seed points). Moreover, fiber tracking results should be compared with those of other approaches, such as for example probabilistic ones. Ultimately, this work should help clinicians in better understanding the precision of generated fiber tracking results.

## ACKNOWLEDGMENTS

The authors would like to thank Dr. Benjamin Geisler for the insightful discussions on locating and tracking the corticospinal tract in the human brain. This project was funded in part by the German Research Society (DFG PE199/21-1).



## REFERENCES

- [1] Lori, N.F. and Akbudak, E. and Shimony, J.S. and Cull, T.S. and Snyder, A.Z. and Guillory, R.K. and Conturo, T.E. “Diffusion tensor fiber tracking of human brain connectivity: acquisition methods, reliability analysis and biological results” *NMR in Biomedicine*, Vol. 15, pp.493–515, 2002
- [2] Göschl, C. and Fahrmeir, L. and Pütz, B. and Auer, L.M. and Auer, D.P. “Fiber tracking from DTI using linear state space models: detectability of the pyramidal tract” *NeuroImage*, Vol. 16, pp.378–388, 2002
- [3] Fieremans, E. and De Deene, Y. and Delputte, S. and Ozdemir, M.S. and D’Asseler, Y. and Vlassenbroeck, J. and Deblaere, K. and Achten, E. and Lemahieu, I. “Simulation and experimental verification of the diffusion in an anisotropic fiber phantom” *Journal of Magnetic Resonance*, Vol. 190(1), pp.189–199, 2008
- [4] Assaf, Y. and Freidlin, R. Z. and Rohde, G. K. and Basser, P. J. “New modeling and experimental framework to characterize hindered and restricted water diffusion in brain white matter” *Magnetic Resonance in Medicine*, Vol. 52, pp. 965–978, 2004
- [5] Assaf, Y. and Basser, P. J. “Composite hindered and restricted model of diffusion (CHARMED) MR imaging of the human brain” *NeuroImage*, Vol. 27, pp. 48–58, 2005
- [6] Gudbjartsson, H. and Patz, S. “The Rician distribution of noisy MRI data” *Magnetic Resonance in Medicine*, Vol. 34, pp. 910–914, 1995
- [7] Hahn, H.K. and Klein, J. and Nimsky, C. and Rexilius, J. and Peitgen, H.-O. “Uncertainty in diffusion tensor based fiber tracking” *Acta Neurochirurgica*, Suppl. 98, pp. 33–41, 2006
- [8] Collins, A.P. and Zijdenbos, A.P. and Kollokian, V. and Sled, J.G. and Kabani, N.J. and Holmes, C.J. and Evans, A.C. “Design and construction of a realistic digital brain phantom” *Transactions on Medical Imaging*, Vol. 17(3), pp. 463–468, 1998
- [9] Holmes, C. and Hoge, R. and Collins, D. and Woods, R. and Toga, A. and Evans, A. “Enhancement of MR images using registration for signal averaging” *J. Comput. Assist. Tomogr.*, Vol. 22, pp. 324–333, 1998
- [10] Pierpaoli, C. and Jezzard, P. and Basser, P.J. and Barnett, A. and Di Chiro, G. “Diffusion tensor MR imaging of the human brain” *Radiology*, Vol. 201, pp. 637–648, 1996
- [11] Bhagat, Y. A. and Beaulieu, C. “Diffusion anisotropy in subcortical white matter and cortical gray matter: changes with aging and the role of CSF-suppression” *Magnetic Resonance Imaging*, Vol. 20, pp. 216–227, 2004
- [12] Partridge, S.C. and Mukherjee, P. and Henry, R.G. and Miller, S.P. and Berman, J.I. and Jin, H. and Lu, Y. and Glenn, O.A. and Ferriero, D.M. and Barkovich, A.J. and Vigneron, D.B. “Diffusion tensor imaging: serial quantitation of white matter tract maturity in premature newborns” *NeuroImage*, Vol. 22, pp. 1302–1314, 2004
- [13] Leemans, A. and Sijbers, J. and Verhoye, M. and Van der Linden, A. and Van Dyck, D. “Mathematical framework for simulating diffusion tensor MR neural fiber bundles”, *Magnetic Resonance in Medicine*, Vol. 53, pp. 944–953, 2005
- [14] Parker, D. and Gullberg, G. “Signal-to-noise efficiency in magnetic resonance imaging” *Med.Phys.*, Vol. 17(2), pp. 250–257, 1990
- [15] Zhou, J. and Gullapalli, R.P. “MR artifacts, safety, and quality control” *RadioGraphics*, Vol. 26, pp. 275–297, 2006
- [16] Schlüter, M. and Konrad-Verse, O. and Hahn, H.K. and Stieltjes, B. and Rexilius, J. and Peitgen, H.-O. “White matter lesion phantom for diffusion tensor data and its application to the assessment of fiber tracking” *SPIE Medical Imaging*, Vol. 5746, pp. 835–844, 2005
- [17] Sijbers, J. “Signal and noise estimation from magnetic resonance images” *Ph.D. Thesis*, 1998
- [18] BrainWeb Project: <http://www.bic.mni.mcgill.ca/brainweb/>
- [19] BrainWeb Parameters: [http://www.bic.mni.mcgill.ca/brainweb/tissue\\_mr\\_parameters.txt](http://www.bic.mni.mcgill.ca/brainweb/tissue_mr_parameters.txt)